地形　第33巻第4号
469-484頁　(2012)

JGU Transactions, Japanese Geomorphological Union
33-4, p. 469-484 (2012)

Flume Experiments on Microdelta Formation: Different Mechanism between Silty and Fine-Sandy Grains

Taro SUZUKI[1] and Noritaka ENDO[2]

Abstract

In this study, flume experiments were performed to investigate the trend of change in the topographies of silty microdeltas depending on water discharge, sediment supply rate, and water depth, in comparison with the topographies of microdeltas formed from fine sand. Previous studies have demonstrated that the contact between the foreset and bottomset of sandy and gravelly microdeltas changes from an angular contact to a tangential one as water discharge increases. This behavior was also observed in the present experiment when fine sand was used. However, this study presents a new relationship between the topography of silty microdeltas and water discharge. For silt, a tangential contact, an angular contact, and a second tangential contact appeared in that order with increase in water discharge. Visual observation revealed that the tangential contact in the lower-discharge regime was formed by the combination of laminar density currents and continuous grain flows, whereas that in the higher-discharge regime was generated by grain fall.

Key words: *flume experiment, silty microdelta, sediment transport mode, slope contact, delta profile*

Introduction

The bedforms (e.g., ripples and dunes) generated under unidirectional flows exhibit a deltaic feature. The lee side slope is wedge-shaped in a vertical cross section parallel to the flow, where the flow enters a standing body of deeper water, and the wedge progrades in a manner similar to that of a delta formation at the mouth of a river. A microdelta is a small-scale deltaic topography, usually formed in experimental flumes, that is composed of three areas: an almost horizontal upstream shallow area (the topset), a lee-side slope (the foreset), and a downstream deep and flat area (the bottomset) (Potter and Pettijohn, 1963; Jopling, 1965). Dunes and ripples, especially those having long wavelengths for their height, possess a relatively flat and horizontal part upstream of the deltaic feature; for example, washed-out ripples, formed near the upper-stage

Received September 28, 2011; revised July 14, 2012; accepted August 1, 2012

[1] Graduate School of Earth and Environmental Sciences, Kanazawa University, Kakuma, Kanazawa, Ishikawa 920-1192, Japan; Present address: HOKKOKU CHISUI Corporation, Mikage 25-1, Kanazawa, Ishikawa 921-8021, Japan

[2] School of Natural System, Kanazawa University, Kakuma, Kanazawa, Ishikawa 920-1192, Japan

plane-bed regime, with the crest upstream of the brinkpoint (Baas and De Koning, 1995). A microdelta is an analog of the lee side slope of a bedform that migrates downstream (Jopling, 1965). Bedload sheets over migrating dunes account for the near total amount of sediment transport on the bed that drives dune migration (Allen, 1982; Bridge, 2003; Venditti et al., 2005; Reesink and Bridge, 2007; 2009). When considering the dynamics of superimposed bedload sheets, underlying dunes can be regarded as the background of deltaic topography.

Previous flume experiments have revealed that the foreset profile is determined by various parameters. The foreset becomes gentle and the shape of the contact between the foreset and bottomset changes from an angular contact to a tangential one with increase in flow velocity and/or water discharge on the topset (Jopling, 1965; Kojima and Yokokawa, 1997), as well as with increase in the sediment supply rate (Allen, 1970; 1982; Carling and Glaister, 1987; Okazaki et al., 2004; Reesink and Bridge, 2007; 2009), decrease in grain size (Jopling, 1965; Kostic and Parker, 2003; Okazaki et al., 2004), and with decrease in water depth on the bottomset (Jopling, 1965).

Two different tendencies between the variation in foreset profiles and flow velocity under unidirectional tidal flow have been reported. Kohsiek and Terwindt (1981) investigated the relationship between the velocity of a tidal current and the topographic profiles of modern tidal megaripples (approximately 25 cm in height) composed of 150 – 200 μm mean grains. They reported that the increasing current velocity caused the laminae to change from angular to tangential contacts. Kreisa and Moiola (1986) studied tidal bundles from the Jurassic Curtis Formation, Utah (approximately 40 cm high). These are composed of sand and mud and have been interpreted to be formed by migrating tidal megaripples during a single tide. They concluded that an increase in the velocity of the tidal current caused the laminae to change from tangential to angular contacts. The above two reports conflict with each other. Nevertheless, this conflict has not yet been explained by sedimentological experiments, because to date, experiments investigating deltaic topography considering all relevant parameters such as water discharge, sediment supply rate, water depth, and grain size have not been comprehensively performed. In this study, we conducted flume experiments to produce microdeltas from fine-sandy and silty sediments, and investigated how the topographic profiles of the microdeltas are influenced by the above parameters.

Experiment

Experimental apparatus

Our experimental apparatus is shown schematically in Fig. 1. The experimental flume was formed of transparent acrylic resin, and was 1 m long, 15 cm deep, and 2.7 cm wide; the floor of the flume was horizontal. A chute was placed at the upstream end of the flume to supply water and sediment to it. The chute was 2 m long and constructed from a gutter made of polyvinyl chloride. The chute was set at an incline of

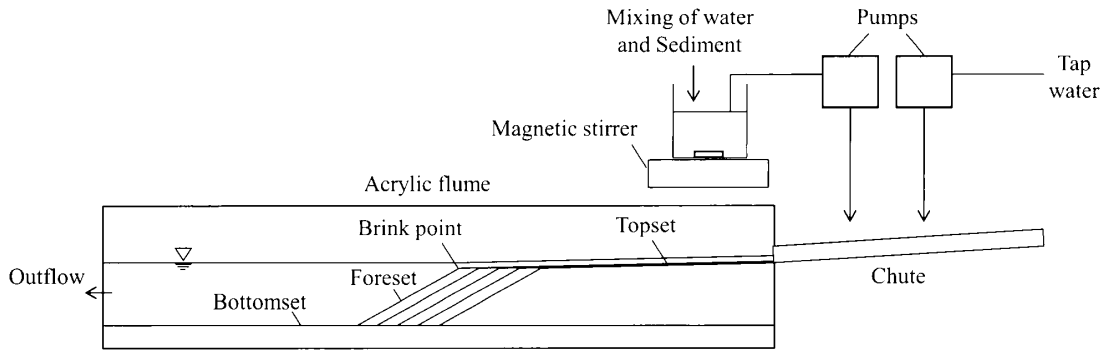

Fig. 1. Schematic of the experimental apparatus.

approximately 5°.

During each run, the mixture of sediment and water was agitated by a magnetic stirrer in a beaker and pumped up into the chute. Tap water was supplied to the chute using the other pump (Fig. 1). Both pumps can supply their water and sediment at a constant rate.

We conducted two series of experiments: one with fine sand and the other with silt. Quartz sand with a mean grain size of 127 μm, density of 2.7 g cm^{-3}, and settling velocity of 1.1 cm s^{-1} was used for the fine sand material. Diatomaceous silt of mean grain size 37.8 μm, density of 2.4 g cm^{-3}, and settling velocity of 8.3×10^{-2} cm s^{-1} was used for the silt. The subaqueous angle of repose for both materials was approximately 34°.

Definition of parameters

The sediment supply rate Q_s is defined as the sediment volume supplied into the flume per minute (cm^3 min^{-1}), which is calculated by $Q_s=Q_tC/\rho_s$, where Q_t is the volume of turbid water supplied into the flume per minute (cm^3 min^{-1}), C is the sediment concentration of the turbid water (g cm^{-3}), and ρ_s is the grain density (g cm^{-3}). The water discharge is the sum of the discharges of tap water and turbid water (cm^3 min^{-1}).

The angle of foreset θ_M is defined as the slope of the straight line connecting the points A and B (Fig. 2), both of which are located on the slope. The heights of points A and B are at 10% and 90% of the height of the slope from the bottom, respectively (Fig. 2a). A foreset slope of less than 25° is called a "gentle slope," whereas a foreset slope more than 25° is called a "steep slope." The slope of the straight line connecting point A with the toe of the slope is called θ_L.

The contact between the foreset and bottomset is classified on the basis of θ_C, i.e., the difference between θ_M and θ_L ($\theta_C=\theta_M-\theta_L$). The contact is called an angular contact when θ_C is less than 5° and called tangential when θ_C is more than 5° (Figs. 2b and 2c).

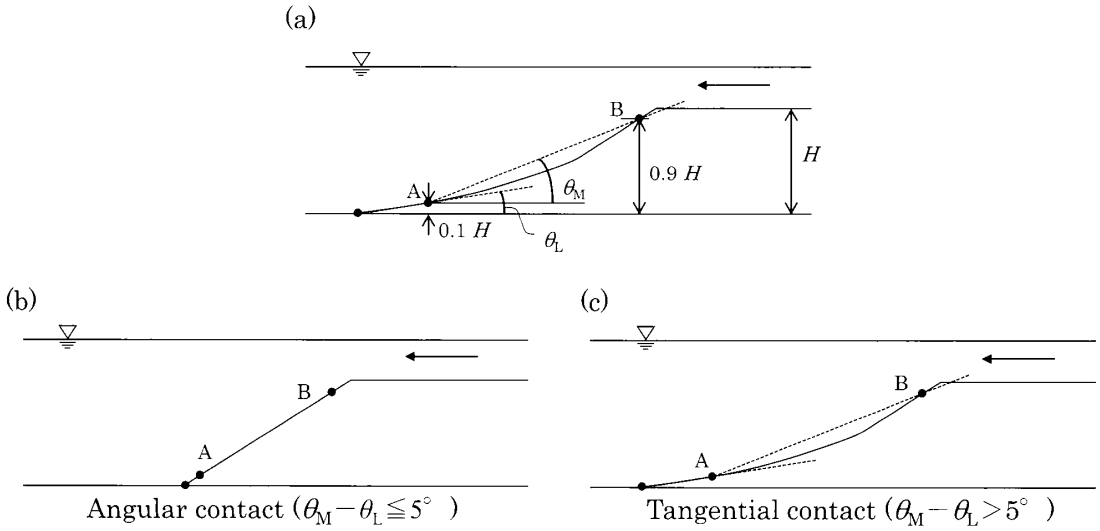

Fig. 2. Schematic illustrations of parameters measured on the foreset slope (a). The slopes are classified according to θ_M as gentle (<25°) or steep (>25°). Schematics of contact types categorized as angular (b) or tangential (c).

Procedure

The experimental setting was prepared as follows. The flume was filled with water to the level of the lowest point of the chute, approximately 10 cm deep. An initial step-like topography was manually formed in the sediment so that the topset surface was at the water level and the brink was approximately 30 cm horizontally downstream as measured from the chute. The bottomset was manually set at a specific depth for each run (Tables 1-4). Water and sediment were supplied from the upstream chute at a specific rate for each run (Tables 1-4). When the water discharge and the sediment

Table 1. Experimental conditions and data for fine-sandy microdeltas when water depth at the bottomset was 2.4 - 5.0 cm.

No.	Water discharge [$cm^3\ min^{-1}$]	Sediment supply rate [$cm^3\ min^{-1}$]	Water depth on the bottomset [cm]	Water depth on the topset [cm]	θ_M [°]	Gradients of forset slope	θ_L [°]	θ_C [°]	Contact between the foreset and the bottomset
Ss-1	200	1.1	3.1	0.2	32.0	Steep	32.1	− 0.1	Angular
Ss-2	200	1.9	3.1	0.1	31.4	Steep	31.4	0.0	Angular
Ss-3	400	1.0	3.0	0.2	33.2	Steep	32.5	0.7	Angular
Ss-4	2100	0.0	2.4	0.5	31.6	Steep	32.5	− 0.9	Angular
Ss-5	2100	1.9	3.0	0.5	32.0	Steep	32.9	− 0.9	Angular
Ss-6	2800	1.9	2.9	0.9	31.4	Steep	3.4	28.0	Tangential
Ss-7	5100	0.0	2.5	1.0	32.2	Steep	5.2	27.0	Tangential
Ss-8	5100	1.9	2.6	1.1	30.6	Steep	4.7	25.9	Tangential
Ss-9	6000	0.0	3.1	1.1	29.8	Steep	4.6	25.2	Tangential
Ss-10	6000	1.9	2.9	1.0	26.8	Steep	4.5	22.3	Tangential
Ss-11	5000	1.1	5.0	1.1	32.8	Steep	34.4	− 1.6	Angular
Ss-12	8000	1.1	5.0	1.1	32.4	Steep	2.7	29.8	Tangential

Table 2. Experimental conditions and data for fine-sandy microdeltas when water depth at the bottomset was 6.3 - 7.9 cm.

No.	Water discharge [cm^3 min^{-1}]	Sediment supply rate [cm^3 min^{-1}]	Water depth on the bottomset [cm]	Water depth on the topset [cm]	θ_M [°]	Gradients of forset slope	θ_L [°]	θ_C [°]	Contact between the foreset and the bottomset
Sd-1	200	1.1	6.7	0.1	32.6	Steep	32.6	0.0	Angular
Sd-2	1000	1.9	7.6	0.3	32.0	Steep	31.7	0.3	Angular
Sd-3	2100	1.1	6.5	0.5	33.9	Steep	33.7	0.2	Angular
Sd-4	2100	9.8	6.3	0.4	32.6	Steep	32.3	0.3	Angular
Sd-5	2700	12.0	7.5	0.4	31.4	Steep	31.5	− 0.1	Angular
Sd-6	3400	12.0	7.5	0.9	32.6	Steep	32.7	− 0.1	Angular
Sd-7	4800	0.0	7.7	1.0	32.4	Steep	32.3	0.1	Angular
Sd-8	5700	1.1	7.9	1.4	32.9	Steep	33.1	− 0.2	Angular
Sd-9	5700	9.8	7.4	1.1	31.7	Steep	33.1	− 1.4	Angular

Table 3. Experimental conditions and data for silty microdeltas when water depth at the bottomset was 2.6 - 5.0 cm.

No.	Water discharge [cm^3 min^{-1}]	Sediment supply rate [cm^3 min^{-1}]	Water depth on the bottomset [cm]	Water depth on the topset [cm]	θ_M [°]	Gradients of forset slope	θ_L [°]	θ_C [°]	Contact between the foreset and the bottomset
Ks-1	200	0.6	3.0	0.2	19.6	Gentle	8.0	11.6	Tangential
Ks-2	200	1.2	2.9	0.2	14.5	Gentle	1.7	12.8	Tangential
Ks-3	400	2.5	2.7	0.2	20.2	Gentle	8.6	11.6	Tangential
Ks-4	400	3.8	2.6	0.2	15.5	Gentle	12.0	3.5	Tangential
Ks-5	600	1.2	3.1	0.3	12.8	Gentle	5.2	7.6	Tangential
Ks-6	600	0.6	3.0	0.3	13.4	Gentle	14.4	− 1.0	Angular
Ks-7	1000	0.6	3.1	0.4	21.2	Gentle	18.5	2.7	Angular
Ks-8	1000	1.2	3.0	0.5	13.5	Gentle	17.2	− 3.7	Angular
Ks-9	1400	1.2	3.0	1.0	20.2	Gentle	18.7	1.5	Angular
Ks-10	1400	0.6	3.1	0.6	25.3	Steep	22.5	1.8	Angular
Ks-11	2000	0.6	3.1	1.0	29.4	Steep	4.3	25.1	Tangential
Ks-12	2000	1.2	2.9	0.8	28.3	Steep	3.7	24.6	Tangential
Ks-13	2800	0.6	3.0	1.2	28.4	Steep	4.0	24.4	Tangential
Ks-14	2800	1.2	3.0	1.2	29.9	Steep	3.4	26.5	Tangential
Ks-15	3700	0.6	2.9	1.4	28.0	Steep	2.1	25.9	Tangential
Ks-16	3700	1.2	3.0	1.4	29.8	Steep	2.9	26.9	Tangential
Ks-17	4800	0.6	3.0	1.9	27.0	Steep	5.9	21.1	Tangential
Ks-18	4800	1.2	3.1	1.2	26.0	Steep	4.9	21.1	Tangential
Ks-19	5900	1.3	3.7	1.6	28.4	Steep	5.9	22.5	Tangential
Ks-20	3000	1.3	5.0	1.2	29.3	Steep	31.4	− 2.1	Angular
Ks-21	5000	1.3	5.0	1.7	28.1	Steep	24.8	3.3	Angular
Ks-22	6000	1.3	5.0	1.9	25.2	Steep	5.1	20.1	Tangential

Table 4. Experimental conditions and data for silty microdeltas when water depth at the bottomset was 5.7 - 8.5 cm.

No.	Water discharge [cm^3 min^{-1}]	Sediment supply rate [cm^3 min^{-1}]	Water depth on the bottomset [cm]	Water depth on the topset [cm]	θ_M [°]	Gradients of forset slope	θ_L [°]	θ_C [°]	Contact between the foreset and the bottomset
Kd-1	200	1.3	7.7	0.1	15.8	Gentle	9.9	5.9	Tangential
Kd-2	200	2.0	7.4	0.2	11.4	Gentle	4.8	6.6	Tangential
Kd-3	200	3.6	7.4	0.2	9.8	Gentle	3.2	6.6	Tangential
Kd-4	262	0.9	7.3	0.2	24.9	Gentle	14.7	10.2	Tangential
Kd-5	400	3.8	7.1	0.2	20.7	Gentle	15.5	5.2	Tangential
Kd-6	533	3.3	6.9	0.2	24.2	Gentle	15.7	8.5	Tangential
Kd-7	600	3.6	7.0	0.3	24.3	Gentle	18.8	5.5	Tangential
Kd-8	200	0.4	7.6	0.3	27.1	Steep	26.1	1.0	Angular
Kd-9	400	0.4	7.0	0.4	26.9	Steep	26.4	0.5	Angular
Kd-10	400	1.3	6.0	0.3	28.4	Steep	27.2	1.2	Angular
Kd-11	400	2.0	6.5	0.3	27.8	Steep	25.7	2.2	Angular
Kd-12	400	2.5	7.2	0.2	27.6	Steep	24.2	3.4	Angular
Kd-13	600	0.7	6.2	0.4	30.4	Steep	27.7	2.7	Angular
Kd-14	600	1.3	5.7	0.2	31.3	Steep	30.5	0.8	Angular
Kd-15	600	2.0	5.8	0.3	29.6	Steep	31.3	- 1.7	Angular
Kd-16	800	1.3	7.2	0.3	29.4	Steep	28.2	1.2	Angular
Kd-17	800	3.3	7.4	0.3	26.4	Steep	28.7	- 2.2	Angular
Kd-18	800	3.6	6.5	0.3	29.3	Steep	25.0	4.3	Angular
Kd-19	2300	0.4	7.0	0.7	28.6	Steep	27.0	1.6	Angular
Kd-20	6000	1.3	8.5	1.9	32.2	Steep	30.2	2.0	Angular

supply rate was steady, the topset surface was kept flat, and the water depth on the topset and the volume of sediment introduced into the system were also kept constant. Under these conditions, the developed microdelta prograded and the foreset slope maintained its shape when the flow conditions on the topset were stable.

The experiments were carried out under different combinations of water discharge (200 - 6000 cm^3 min^{-1}), sediment supply rate (0.5 - 11.9 cm^3 min^{-1}), grain size (37.8 - 127 μm), and water depth at the bottomset (2.4 - 8.5 cm) (Tables 1 - 4). All runs were performed under the steady state. To evaluate the angle of the foreset and to determine the contact types, θ_M and θ_L were measured under the same steady state conditions.

Results and discussion

Topographic profiles in relation to water discharge and sediment supply: in case of fine sand

Table 1 shows the experimental results when fine sand was used with 2.4 - 5.0 cm water depth at the bottomset. For the same depth at the bottomset, angular and tangential contacts appeared at low and high discharge, respectively. All runs in Table 1

resulted in steep slopes ($\theta_M > 25°$).

Figure 3a shows a photograph (upper) and a schematic (lower) of sediment transport when an angular contact with a steep slope was observed (run Ss − 2). Visual observation revealed that the angular contact with a steep slope was formed by the grain flow intermittently running down the foreset slope. The sediment supplied from upstream deposited on the upper part of the slope. The deposition made the upper part of the slope steep and caused avalanches (i.e., grain flow). When the grain flow reached the bottomset, the sediment stopped at its angle of repose. This mechanism of formation of angular contacts was the same as that described by Jopling (1965), Allen (1970), Hunter and Kocurek (1986), Kleinhans (2004), and Reesink and Bridge (2007; 2009).

Visual observation also revealed that a vortex was formed downstream of the slope. When the depth at the bottomset was greater than the height of the vortex, backflows could not affect the lower part of the slope. Therefore, the sand grains moved on the slope only because of gravity (i.e., grain flow), resulting in a microdelta with a steep slope and an angular contact (Fig. 3a schematic).

Figure 3b shows a photograph and a schematic of sediment transport when a tangential contact with a steep slope was formed (run Ss-10). The steep slope was formed by grain flow intermittently running down the upper foreset slope. The tangential contacts in this case were formed by grain fall, i.e., the grains were ejected at the brinkpoint by the separated flow and deposited on the bottomset near the base of the foreset slope. The grains were transported a considerable distance away from the brinkpoint. In this case, the size of the vortex was large enough to affect the bottomset (Fig. 3b schematic). The grains deposited near the contact between the foreset and bottomset by backflows from the vortex made the contact tangential. This mode of tangential contact formation is the same as that described by Allen (1963), Hunter (1977), and Reesink and Bridge (2007; 2009). The backflows observed also reworked the grains deposited on the bottomset and transported them upstream to form regressive ripples, as reported by Jopling (1961; 1965) and Reesink and Bridge (2007; 2009). These ripples promoted the formation of tangential contacts.

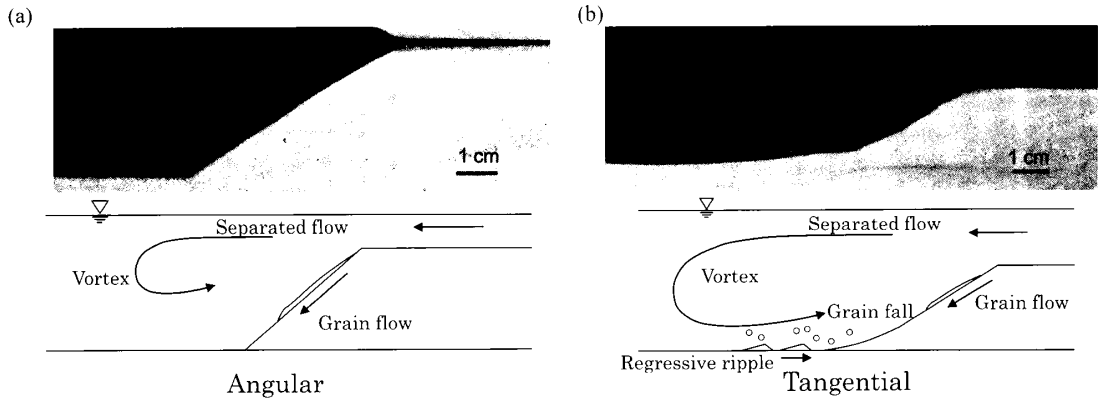

Fig. 3. Photographs and schematic illustrations of transport mode and microdelta shapes for fine sand. The photographs show (a) run Ss-2, (b) run Ss-10.

Figure 4 shows our experimental result for runs at a water depth of approximately 3 cm plotted on a graph of water discharge versus sediment supply rate. The boundary between angular contacts and tangential contacts is also shown. Angular contacts appeared when the discharge was less than 2100 cm^3 min^{-1} (runs Ss-1 to Ss-5), whereas tangential contacts were formed when the discharge was greater than 2800 cm^3 min^{-1} (runs Ss-6 to Ss-10). No correlation was found between the type of contact and the sediment supply rate (Fig. 4).

Table 2 shows our experimental results when fine sand was used with water depth at the bottomset of 6.3 - 7.9 cm. Only angular contacts with steep slopes were formed at these depths (runs Sd-1 to Sd-9). The mechanism of angular contact formation was the same as that observed at shallower water depths of 2.4 - 5.0 cm.

Topographic profiles in relation to water discharge and water depth: in case of fine sand

The experimental results were plotted on a graph of water discharge versus water depth at the bottomset (Fig. 5). Only the data where the sediment supply rate was

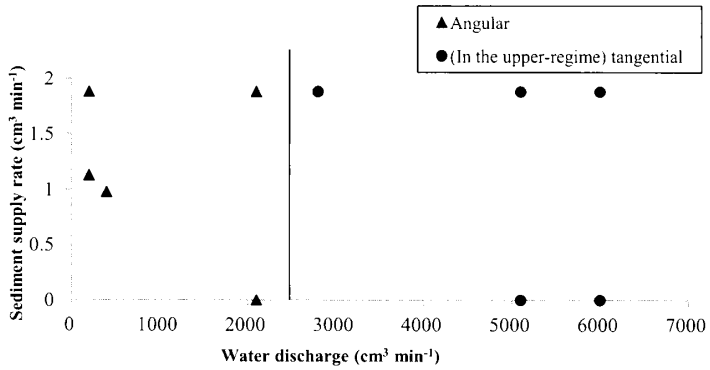

Fig. 4. Plot of fine-sandy microdelta profiles against water discharge and sediment supply rate. Water depth at the bottomset was approximately 3 cm. See text for description of "in the upper-regime."

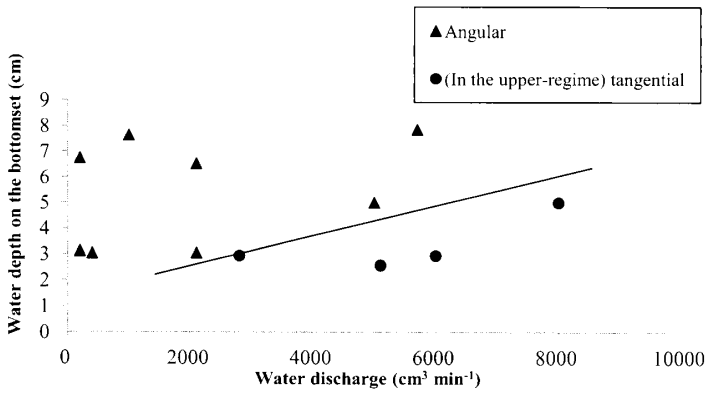

Fig. 5. Plot of fine-sandy microdelta profiles against water discharge and water depth at the bottomset. Only runs with 1 - 2 cm_3 min^{-1} sediment supply rate are plotted. See text for description of "in the upper-regime."

between 1 and 2 cm^3 min^{-1} are plotted, so that we can specifically examine only the effect of water discharge and water depth. The boundary between angular contacts and tangential contacts is also shown. The diagram shows that the contact type changes from angular to tangential with increase in water discharge and with decrease in water depth at the bottomset.

Whether the vortex affects the bottomset depends on the size of vortex relative to the depth at the bottomset. For experimental runs at water discharge of approximately 5,000 – 6,000 cm^3 min^{-1}, only a small amount of sediment is deposited near the contact between the foreset and bottomset beds by the backflows when the bottomset was deep. When the depth at the bottomset was more than the vortex size, the formed microdeltas tended to have angular contacts because the effect of the backflows is small even if the discharge rate is relatively high.

Topographic profiles in relation to water discharge and sediment supply: in case of silt

Table 3 shows experimental results when silt was used with water depth at the bottomset of 2.6 – 5.0 cm. In these experiments, the tangential contact, the angular contact with gentle slope, the angular contact with steep slope, and the tangential contact appeared in this order with increase of water discharge. Hereafter the tangential contacts that appeared at lower discharge are referred to as "lower-regime tangential contact," and the tangential contacts produced at higher discharge are referred to as "upper-regime tangential contacts".

Observations during the formation of the four types of profile clarified that each of these profiles was formed by a combination of different mechanisms. Figure 6 shows photographs and schematics of typical microdelta formation runs for this type of silty sediment.

Figure 6a shows a photograph and a schematic of sediment transport for a lower-regime tangential contact (run Ks-1). Lower-regime tangential contacts were formed by a combination of continuous grain flows and laminar density currents flowing down from the foreset to the bottomset. The laminar density current consisted of suspended particles flowing along the bed owing to the weight of the current itself. The continuous grain flows and laminar density currents proceeded downstream even beyond the contact, thus forming tangential contacts.

Kostic and Parker (2003) and Okazaki et al. (2004) reported that tangential contacts were caused by turbidity currents with increase in sediment supply rate. On the other hand, Reesink and Bridge (2007; 2009) reported that tangential contacts were caused by continuous grain flow with increase in sediment supply rate. However, we did not find any previous experimental studies that described a change from angular contact to tangential contacts with a decrease in water discharge. The present study discovered that, for silt, tangential contacts were formed at discharge smaller than those of the angular contacts. Silts easily run down the slope as laminar density currents because they are easily suspended even if water discharge is small.

Figure 6b shows a photograph and a schematic of sediment transport when an angular contact with a gentle slope was formed (run Ks-8). Angular contacts with a gentle slope were formed by combination of two types of grain motion; a laminar density current and grain flow. The grain flow started from the brinkpoint and grains slid on the foreset as a mass. The laminar density current also started from the brinkpoint, but stopped at the middle of the foreset slope. In this case, the vortex around the foreset formed a current that travelled up the foreset. This current stopped the laminar density flow in the middle of the slope and grain flow in the lower slope. We did not find any examples of this type of angular microdelta formation described in previous studies.

Figure 6c and 6d show photographs and schematics for sediment transport where contacts with steep slopes were produced. Runs Ks-10, Ks-20, and Ks-21 resulted in angular contacts with steep slope whereas runs Ks-11 to Ks-19 and run Ks-22 produced steep upper-regime tangential contacts. These contact types were formed by the same mechanisms that formed the contacts in runs Ss-1 to Ss-5 (grain flow) and runs Ss-6 to Ss-10 (grain fall).

The different types of contacts produced by the silt experimental runs at the bottomset depths of 2.6 to 5.0 cm were plotted on a graph of water discharge versus sediment supply rate (Fig. 7a). Figure 7a shows that lower-regime tangential contacts

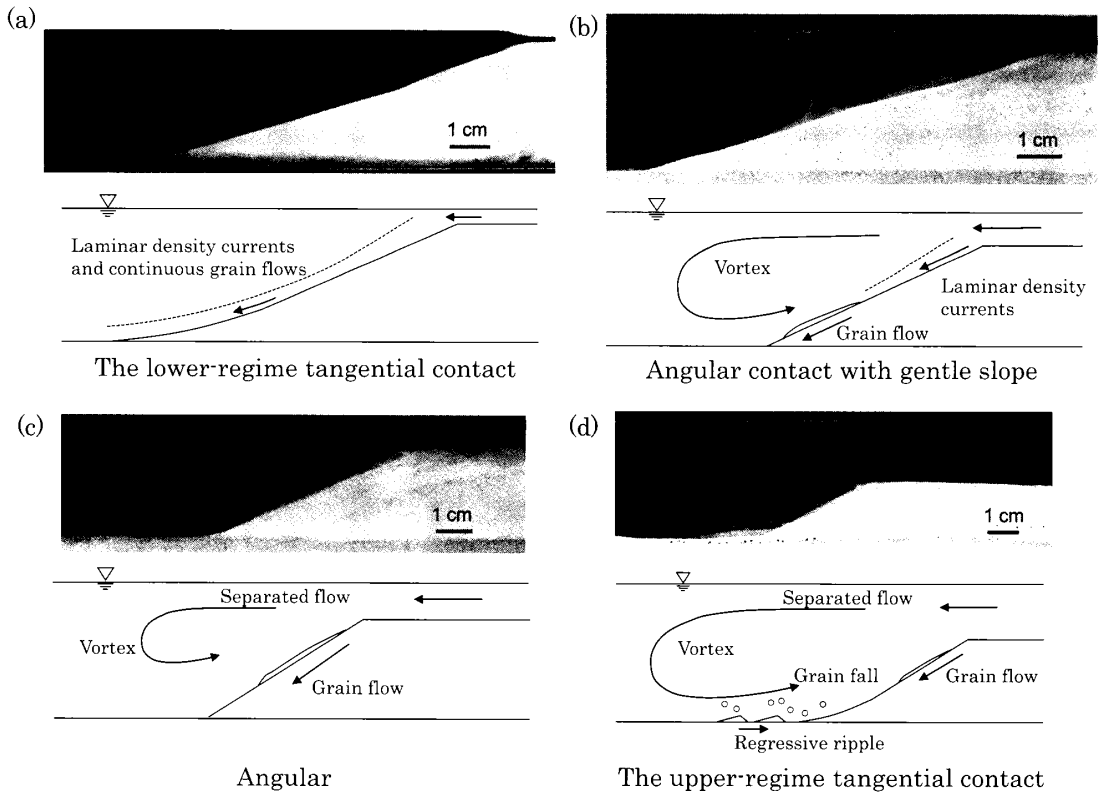

Fig. 6. Photographs and schematic illustrations of transport mode and microdelta shapes for silt. The photographs show (a) run Ks-1, (b) run Ks-8, (c) run Ks-10, and (d) run Ks-18.

appeared at lower water discharge, and that if compared with the same water discharge, lower-regime tangential contacts appeared at higher sediment supply rates. No relationship was found between the appearances of upper-regime tangential contacts and sediment supply rate in the data collected to date (Fig. 7a).

Table 4 shows experimental results obtained when silt was used with water depth at the bottomset of 5.7 – 8.5 cm. In these runs, only tangential contacts with a gentle slope (Kd-1 to Kd-7) and angular contacts with a steep slope were produced (Kd-8 to Kd-20). These two types of contacts were formed by the same mechanisms that formed the contacts in runs Ks-1 through Ks-5 and run Ks-10.

Figure 7b shows contact types in relation to water discharge and sediment supply rate for runs Kd-1 to Kd-20. The figure also shows that tangential contacts with a gentle slope were produced at lower water discharge and were formed at higher sediment supply rates if compared with the same water discharge. As described previously, these contacts resulted from laminar density currents and continuous grain flow.

Angle of foreset and type of contacts are shown in Fig. 8 for all runs in Table 4

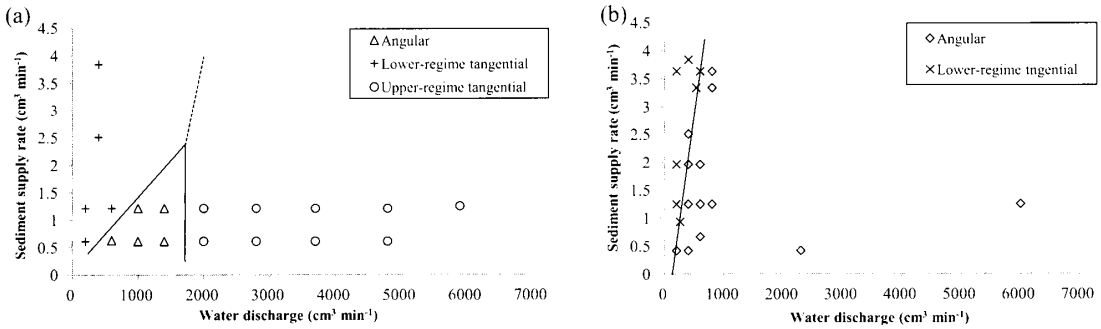

Fig. 7. Plot of silty microdelta profiles against water discharge and sediment supply rate. Water depth at the bottomset was (a) approximately 3 cm and (b) approximately 7 cm. The lines shown are only illustrative demarcations of the types of contacts.

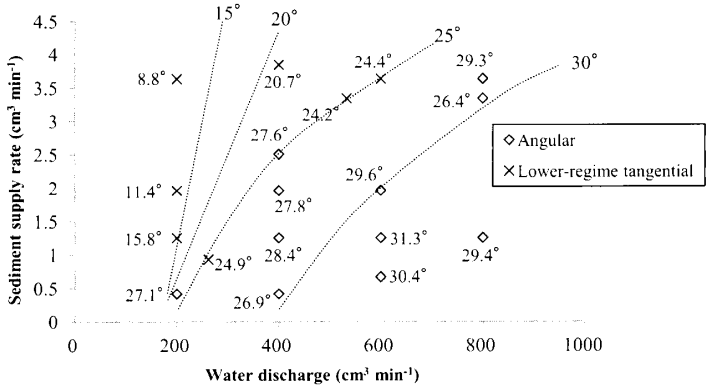

Fig. 8. Gradient of the foreset of silty microdelta against water discharge and sediment supply rate.

except runs Kd-19 and Kd-20, which are off-scale due to high water discharge values. Figure 8 shows that the slope of the foresets changes from approximately 9° to approximately 30° with increase in water discharge and decrease in sediment supply rates.

The gentle slopes (< 25°) were formed by laminar density currents and continuous grain flow. From visual observations, the depocenter of the laminar density currents and continuous grain flows was located downstream of the depocenter for the intermittent grain flows, so the gradient of the foresets became gentler than the angle of repose.

With increase in water discharge, the predominant sediment transport mode on the slope changed from a combination of laminar density currents and continuous grain flows to intermittent grain flow; steep slopes (>25°) formed as a result. The amount of silt supplied to the upper part of the foreset slope decreased when the water discharge increased under conditions of constant sediment supply, because the separated flow strengthened with increase in discharge. The large inertia of grains due to the high discharge caused an increase in the amount of silt transported as a suspended load within the separated flow and a corresponding decrease in the amount of silt supplied to the upper part of the foreset slope. This resulted in weakened laminar density currents.

Topographic profiles in relation to water discharge and water depth: in case of silt

Figure 9 shows three slope-contact types for silty sediment plotted against water discharge and water depth at the bottomset. Here the data plotted are limited to those runs with a sediment supply rate of 1 - 2 cm^3 min^{-1} to isolate the effect of water discharge and water depth. When the depth was 2.6 - 5.0 cm, the contact type changed from lower-regime tangential through angular to upper-regime tangential contacts with increase in water discharge, whereas at depths of 5.7 - 8.5 cm, only the lower-regime tangential contacts and angular contacts appeared.

For silt, whether the upper-regime tangential contacts appear depends on the size of the vortex relative to the water depth at the bottomset. This is identical to the behavior

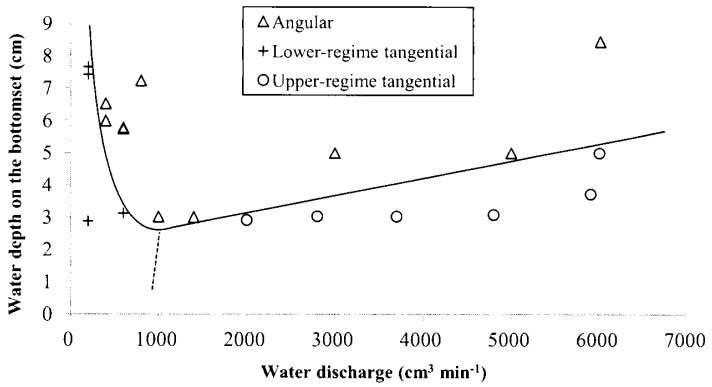

Fig. 9. Plot of silty microdelta profiles against water discharge and water depth at the bottomset. Only runs with 1 - 2 cm^3 min^{-1} of sediment supply rate are plotted to see the dependence of water discharge only.

of the sediment-water system in the case of the fine-sandy microdelta with a water depth of approximately 3 cm described previously. Whether the lower-regime tangential contacts appear depends on how far the laminar density current runs down the foreset slopes relative to the water depth at the bottomset. When the slope is long, the sediment transport modes change from laminar density currents to grain flow at the lower part of the slope owing to the deposition of suspended grains. Therefore, microdeltas with deeper bottomsets (longer slopes) tend to have angular contact even if the discharge is relatively low (Fig. 9).

Comparison of this study to previous studies

Two previous studies, by Kreisa and Moiola (1986) and Kohsiek and Terwindt (1981), have reached contradictory conclusions. Kreisa and Moiola (1986) concluded that the change in cross stratification from tangential contacts with gentle slopes to angular contacts with steep slopes was caused by an increase in flow velocity. They reported that as flow velocity increased, the lee slope of the megaripples steepened, grain flow became predominant, and flow separation and a lee side vortex developed. On the contrary, Kohsiek and Terwindt (1981) interpreted that the change in the topography they observed was from angular contacts with a steep slope to tangential contacts with a gentle slope and was also caused by an increase in flow velocity, but attributed the change to an increasing proportion of grain fall versus grain flow for the sedimentation on the lee side of the megaripple. Furthermore, they attributed it to the growing importance of the vortex and the associated strength of the backflow with increasing current velocity.

The present study might explain the apparent contradiction in the previous studies. The lower-regime tangential contact described in this experiment might correspond to the tangential contact reported by Kreisa and Moiola (1986) and the upper regime tangential contact might correspond to that reported by Kohsiek and Terwindt (1981). The change from the tangential contacts to angular contacts reported by Kreisa and Moiola (1986) is thought to be caused by the same mechanisms that caused the change from lower-regime tangential contacts to angular contacts discovered by this study. In contrast, the change from the angular contacts to tangential contacts reported by Kohsiek and Terwindt (1981) could arise from the same conditions that caused the change from angular contacts to the upper-regime tangential contacts found in this study.

The key difference between the two sets of megaripples discussed above is grain size. The sediments in the tidal bundles reported by Kreisa and Moiola (1986) were mud and sand, whereas the mean grain size of the megaripples of Kohsiek and Terwindt (1981) was sand size. Our experimental results suggest that lower-regime tangential contact could have easily been formed in the sediments that now make up the strata studied by Kreisa and Moiola (1986) because of the fine grain size.

Conclusion

This study revealed a new relationship between the topography of silty microdeltas and water discharge. Lower-regime tangential contacts, angular contacts, and upper-regime tangential contacts can all appear with increase in water discharge. The lower-regime tangential contacts appeared only when silt was supplied. These lower-regime tangential contacts were generated by laminar density currents. Upper-regime tangential contacts appeared for both silt and fine sand. The present study may resolve the apparent contradiction between two previous studies of tidal megaripples.

Acknowledgment

One of the authors, Noritaka Endo, was financially supported by the Japanese Ministry of Education, Culture, Sports, Science and Technology Grant-in-Aid for Young Scientists (B), 19740313, 2007.

References

Allen, J. R. L. (1963) Sedimentation to the lee of small underwater sand waves, an experimental study: Journal of Geology, **73**, 95–116.

Allen, J. R. L. (1970) The avalanching of granular solids on dune and similar slopes: Journal of Geology, **78**, 326–351.

Allen, J. R. L. (1982) Sedimentary structures, their character and physical basis, volume 2: Developments in Sedimentology, **30** b.

Baas, J. H. and De Koning, H. (1995) Washed-out ripples: their equilibrium dimensions, migration rate, and relation to suspended-sediment concentration in very fine sand: Journal of Sedimentary Research, **A65**, 431–435.

Bridge, J. S. (2003) Rivers and floodplains; forms, processes and sedimentary record: Blackwell Publishing, Oxford.

Carling, P. A. and Glaister, M. S. (1987) Rapid deposition of sand and gravel mixtures downstream of a negative step: the role of matrix-infilling and particle-overpassing in the process of bar-front accretion: Journal of the Geological Society, London, **144**, 543–551.

Hunter, R. E. (1977) Basic types of stratification in small eolian dunes: Sedimentology, **24**, 361–387.

Hunter, R. E. and Kocurek, G. (1986) An experimental study of subaqueous slipface deposition: Journal of Sedimentary Petrology, **56**, 387–394.

Jopling, A. V. (1961) Origin of regressive ripples explained in terms of fluid-mechanic processes: Short Papers in Geology and Hydrology Science, U.S. Geological Survey Professional Paper 424-D, 15–17.

Jopling, A. V. (1965) Hydraulic factors controlling the shape of laminae in laboratory deltas: Journal of Sedimentary Petrology, **35**, 777–791.

Kleinhans, M. G. (2004) Sorting in grain flows at the lee side of dunes: Earth-Science Reviews, **65**, 75–102.

Kohsiek, L. H. M. and Terwindt, J. H. J. (1981) Characteristics of foreset and topset bedding in megaripples related to hydrodynamic conditions on an intertidal shoal: Special Publication no. 5, International Association of Sedimentologists, 27–37.

Kojima, I. and Yokokawa, M. (1997) Experimental study on depositional process on micro-delta foreset: Abstracts of the 104th Annual Meeting of the Geological Science of Japan, 318 (in Japanese).

Kostic, S. and Parker, G. (2003) Progradational sand-mud deltas in lakes and reservoirs: Part 2. Experiment and Numerical Simulation: Journal of Hydraulic Research, **41**, 141–152.

Kreisa, R. D. and Moiola, R. J. (1986) Sigmoidal tidal bundles and other tide-generated sedimentary structures of the Curtis Formation, Utah: Geological Society of America Bulletin, **97**, 381–387.

Okazaki, H., Ikeda, H., Mokudai, K. and Iizima, H. (2004) Fundamental experiments foresetimation of process of the Pleistocene delta foresets: Bulletin of the Terrestrial Environment Research Center, **5**, 41–50 (in Japanese).

Potter, P. E. and Pettijohn, F. J. (1963) Paleocurrents and basin analysis: New York, Academic Press Inc., 296.

Reesink, A. J. H. and Bridge, J. S. (2007) Influence of superimposed bedforms and flow unsteadiness on formation of cross strata in dunes and unit bars: Sedimentary Geology, **202**, 281–296.

Reesink, A. J. H. and Bridge, J. S. (2009) Influence of bedform superimposition and flow unsteadiness on the formation of cross strata in dunes and unit bars – Part 2, further experiments: Sedimentary Geology, **222**, 274–300.

Venditti, J. G., Church, M. and Bennett, S. J. (2005) Morphodynamics of small-scale superimposed sand waves over migrating dune bed forms: Water Resources Research, **41**, W10423.

シルト質マイクロデルタの縦断面形状に関する水路実験：流量，土砂供給速度，水深の依存性

鈴木太郎[1]・遠藤徳孝[2]

要　　旨

マイクロデルタの縦断面形の，流量及び砕屑物供給速度，水深に対する依存性に関して水路実験を行い，シルトと細粒砂の場合で比較した．細粒砂の場合，先行研究と同様に，流量の増加に伴いスロープ・コンタクト（フォーセットとボトムセットの境界）はアンギュラー型からタンジェンシャル型に変化した．一方，シルトを用いた場合は，マイクロデルタの斜面形状の変化傾向が，細粒砂の場合と異なることを発見した．シルト質マイクロデルタは，流量の増加に伴いタンジェンシャル型からアンギュラー型を経て再びタンジェンシャル型に変化した．高流量域で発生するタンジェンシャル型は，浮遊した粒子が剥離渦の戻り流れによりスロープ・コンタクトに堆積することで形成された．低流量域で発生するタンジェンシャル型は，密度流と連続的に流下する粒子流が粒子をスロープ・コンタクトへ運搬することで形成された．

[1] 金沢大学大学院自然科学研究科地球環境学専攻
[2] 金沢大学理工研究域自然システム学系